(2)

NAVAL POSTGRADUATE SCHOOL
Monterey, California

THESIS

A COMPARISON OF HIGH LATITUDE IONOSPHERIC PROPAGATION PREDICTIONS FROM IONCAP-PC 2.5 WITH MEASURED DATA

by

Marcos D. Tsolekas

December 1990

Thesis Advisor: Richard W. Adler

Approved for public release; distribution is unlimited.

REPORT DOCUMENTATION PAGE

Form Approved OMB No. 0704-0188

1. REPORT SECURITY CLASSIFICATION: Unclassified	1b. RESTRICTIVE MARKINGS
2a. SECURITY CLASSIFICATION AUTHORITY	3. DISTRIBUTION/AVAILABILITY OF REPORT: Approved for public release; distribution is unlimited
2b. DECLASSIFICATION/DOWNGRADING SCHEDULE	
4. PERFORMING ORGANIZATION REPORT NUMBER(S)	5. MONITORING ORGANIZATION REPORT NUMBER(S)
6a. NAME OF PERFORMING ORGANIZATION: Naval Postgraduate School; 6b. OFFICE SYMBOL (If applicable): EC	7a. NAME OF MONITORING ORGANIZATION: Naval Postgraduate School
6c. ADDRESS (City, State, and ZIP Code): Monterey, CA 93943-5000	7b. ADDRESS (City, State, and ZIP Code): Monterey, CA 93943-5000
8a. NAME OF FUNDING/SPONSORING ORGANIZATION; 8b. OFFICE SYMBOL (If applicable)	9. PROCUREMENT INSTRUMENT IDENTIFICATION NUMBER
8c. ADDRESS (City, State, and ZIP Code)	10. SOURCE OF FUNDING NUMBERS: PROGRAM ELEMENT NO. / PROJECT NO. / TASK NO. / WORK UNIT ACCESSION NO.

11. TITLE (Include Security Classification)
A Comparison of High Latitude Ionospheric Propagation Predictions from IONCAP-PC2.5 with Measured Data

12. PERSONAL AUTHOR(S)
Marcos D. Tsolekas

13a. TYPE OF REPORT	13b. TIME COVERED	14. DATE OF REPORT (Year, Month, Day)	15. PAGE COUNT
Master's Thesis	FROM _____ TO _____	December 1990	60

16. SUPPLEMENTARY NOTATION
The views expressed in this thesis are those of the author and do not reflect the official policy or position of the Department of Defense or the U.S. Government.

17. COSATI CODES			18. SUBJECT TERMS (Continue on reverse if necessary and identify by block number)
FIELD	GROUP	SUB-GROUP	High Frequency (HF); Ionospheric Propagation

19. ABSTRACT (Continue on reverse if necessary and identify by block number)

Prediction of ionospheric propagation in polar regions tends to be difficult because of an increased number and variety of local ionospheric disturbances. Various programs have been developed to model ionospheric propagation, and one such program, IONCAP-PC 2.5, is tested for accuracy over a transpolar communications link, using noncentric measured reference data obtained from the Univercity of Leicester.

The field strength values predicted by IONCAP-PC 2.5 are extended to take into consideration the specific antenna designs, and predicted noise levels are also calculated for the environments involved. The resulting signal-to-noise ratio is compared with the observed signal-to-noise ratio, and a statistical analysis is performed on the resulting errors.

It is concluded that IONCAP-PC 2.5 predicts the signal-to-noise ratio with an error of less than 10 dB for 50% of the data. However, significant errors occur when predicting extreme values for this noncentric data.

20. DISTRIBUTION/AVAILABILITY OF ABSTRACT	21. ABSTRACT SECURITY CLASSIFICATION	
☒ UNCLASSIFIED/UNLIMITED ☐ SAME AS RPT. ☐ DTIC USERS	Unclassified	
22a. NAME OF RESPONSIBLE INDIVIDUAL: Richard W. Adler	22b. TELEPHONE (Include Area Code): (408) 646-2352	22c. OFFICE SYMBOL: EC/Ab

DD Form 1473, JUN 86 *Previous editions are obsolete*

Approved for public release; distribution is unlimited.

A Comparison of High Latitude Ionospheric Propagation Predictions from IONCAP-PC 2.5 With Measured Data

by

Marcos D. Tsolekas
Lieutenant, Hellenic Navy
B.S., Hellenic Naval Academy, 1980

Submitted in partial fulfillment of the
requirements for the degree of

MASTER OF SCIENCE IN ELECTRICAL ENGINEERING

from the

NAVAL POSTGRADUATE SCHOOL
December 1990

Author: _____
Marcos D. Tsolekas

Approved by: _____
Richard W. Adler, Thesis Advisor

_____
Stephen Jauregui, Second Reader

_____
Michael A. Morgan, Chairman,
Department of Electrical and Computer Engineering

ABSTRACT

Prediction of ionospheric propagation in polar regions tends to be difficult because of an increased number and variety of local ionospheric disturbances. Various programs have been developed to model ionospheric propagation, and one such program, IONCAP-PC 2.5, is tested for accuracy over a transpolar communications link, using noncentric measured reference data obtained from the Univercity of Leicester.

The field strength values predicted by IONCAP-PC 2.5 are extended to take into consideration the specific antenna designs and predicted noise levels are also calculated for the environments involved. The resulting signal-to-noise ratio is compared with the observed signal-to-noise ratio and a statistical analysis is performed on the resulting errors.

It is concluded that IONCAP-PC 2.5 predicts the signal-to-noise ratio with an error of less than 10 dB for 50% of the data. However, significant errors occur when predicting extreme values for this noncentric data.

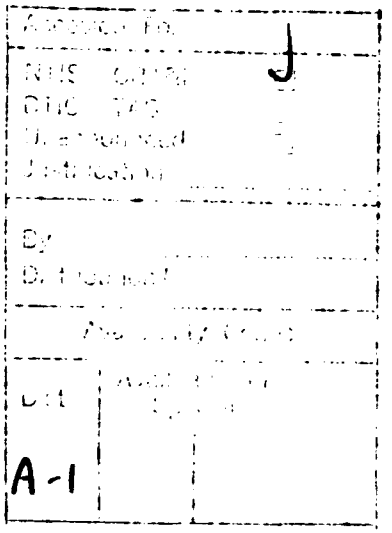

TABLE OF CONTENTS

LIST OF FIGURES

LIST OF TABLES

I. INTRODUCTION

In recent years, satellite data has made a more in-depth analysis of the makeup and behavior of the ionosphere possible. In particular, satellite-based measurements have aided in understanding ionospheric disturbances at high latitudes. These disturbances are connected with solar activities, interactions between the ionosphere and the Earth's magnetosphere, and other physical phenomena for which no explanation is available.

In addition to efforts to explain mechanisms controlling ionospheric behavior, empirical and mathematical prediction models have been developed. Empirical models have been developed which attempt to relate electromagnetic (EM) wave time delay and attenuation to other factors such as the season, height, sunspot number and magnetic activity using previously-collected data. In addition, mathematical models have been developed of the equations of momentum, continuity, and heat flow using numerical methods.

Based on these models, ionospheric propagation prediction programs can predict Maximum Usable Frequency (MUF), field strength, propagation modes, and angles of departure and arrival. Because many of the parameters involved are unknown, it is impossible for the prediction programs to be very accurate. In addition, with transpolar communications links (those that pass through polar regions), ionospheric models tend to be weak, yielding even less accurate predictions.

A. SCOPE OF THESIS

In this thesis, the results of an ionospheric propagation prediction computer program, Ionospheric Communications Analysis and Prediction program (IONCAP), are compared to measured data from a transpolar communication link. In 1948, the Central Radio Propagation Laboratory (CRPL) published a treatise on ionospheric propagation. Based on this document, manual techniques were developed analyzing HF ionospheric circuits of short, intermediate, and long distances. IONCAP is a direct descendent of these techniques (Ref. 1). It was developed by the Institute for Telecommunication Sciences (ITS) in Boulder, Colorado and has proved to be a useful, long-term, ionospheric predictor for middle-latitude communication links. The version used in this study is IONCAP-PC 2.5

A large database, with identification name "noncentric", from the University of Leicester, UK, was available as a reference for the test (Ref. 2). From this database, two campaigns (summer '88, winter '89) with more than 2,200 samples were used for comparison with the predicted values from IONCAP-PC 2.5. The database includes received signal levels, noise levels, and spread index for thirteen frequencies in the HF spectrum on an hourly base for both campaigns. The signal and noise levels are related to, but are not the same, as signal strength and noise power respectively. An RF distribution system was used between the receving antenna and the receivers. The additional noise and interference of this system was unknown so the terms "signal" and "noise levels", were used in the study instead of "signal strength" and "noise power". Each campaign lasted 25 days. The data were categorized according to their reliability by using a spread index (SI) and call sign (CS) test.

Only data which passed both tests will be used for comparison to the data predicted by IONCAP.

B. ANTENNA MODELING

The antennas at the transmitting and the receiving positions have also been analyzed and their performance parameters were incorporated into the prediction program. The transmitting antenna for the summer '88 campaign was a modified Butternut trap-vertical monopole and for the winter '89 campaign an elevated loaded whip. Both were modeled using the Numerical Electromagnetics Code (NEC) using geometry from the University of Leicester (Ref. 3). Patterns for the receive antenna, an inverted vee (the same for both campaigns), were obtained from Ref. 4. The transmitting antennas were located at Clyde River, Canada (70° 28' N , 68° 36' W) and the receiving antenna at Leicester, UK (52° 39' N, 01° 08' W).

C. ANALYSIS OF DATA

The evaluation of IONCAP prediction is based on measuring the error of signal-to-noise ratio (SNR) between predicted and noncentric data for six frequencies of each campaign. The frequencies were selected in order to include as much data as possible and also to represent a reasonable sample of the HF spectrum. Because IONCAP predicts the noise power at the receiver for 1 Hz bandwidth at 3 MHz, it was calculated manually for the specific bandwidth (50 Hz) of the fast Fourier transform (FFT) used by the UK researchers. The statistical analysis of the error is based on a method developed by Professor A. Tomko of Johns Hopkins University (Ref. 5).

II. PREDICTION MODEL DESCRIPTION

The prediction model is based on IONCAP but also uses input data from other sources for additional accuracy.

A. IONCAP

Manual ionospheric propagation prediction methods have existed since 1948. These methods were laborious and time consuming and were used sparingly. The IONCAP computer program is a direct descendant of these manual methods. It is based on an empirical ionospheric model with a ray tracing routine, as well as a noise model. It is written in FORTRAN and its modular form permits modifications to individual sections without affecting other sections. The seven independent sections are:

- input,
- path geometry,
- antennas,
- ionospheric parameters,
- maximum usable frequency,
- system performance, and
- output.

The input section consists of three subroutines for card images, long term data tape image, and an antenna tape image. The subroutines produce parameters for control run options, numeric coefficients for ionospheric parameters, and optional antenna patterns.

The path geometry section determines the circuit geometry and evaluates the Earth's magnetic field at selected sample areas of the path. Antenna subroutines process antenna data and calculate antenna gains and patterns.

The ionospheric parameter section evaluates the ionospheric parameters using an explicit electron-density profile. It evaluates these parameters for D, E and F2 regions, an F1 ledge and an E-F valley. The maximum usable frequency section evaluates the MUF and optimum working frequency (FOT) using a corrected form of Martyn's theorem.

The system performance sections are divided into two sets, one for short distances (less than 10,000 Km) and the other for longer distances. The short path set evaluates each possible ray path. It takes into account high and low angle, E, F1, F2 and sporadic-E modes to the extent possible over the MUF modes. Output subroutines generate output options as line printer images.

1. Data Input Requirements

The data requirements for IONCAP consist of a fixed long-term data base file and user-defined input data. The long-term data base includes geographic and time variations of the ionosphere, propagation path geometry, signal attenuation and theoretical performance of certain antenna systems. It has evolved over many years, incorporating data collected using three basic criteria

- availability on a worldwide basis for time, diurnal, yearly and solar cycles,
- availability of data distribution, and
- consistency between data sets.

The user defined input data includes frequency of operation, sunspot number, antenna type, transmitter power, man-made noise, etc.. For example the user can define up to 11 frequencies for ionospheric prediction performance.

2. Output Options

There are four output subsets in IONCAP:

- ionospheric description,
- antenna patterns,
- MUF predictions, and
- system performance predictions.

From these subsets, system performance predictions (the main output of IONCAP) estimate MUF, median field strength, S/N ratio, main propagating mode, etc. The median field strength of the electric field at the receiving antenna is given in dB referred to one microvolt per meter. It is considered more accurate than the S/N ratio because the latter involves an estimation of noise power. The noise power is estimated for 1 Hz bandwidth at 3 MHz and one must recalculate it for the bandwidth in use.

3. Assumptions

IONCAP simulates the propagation of the EM wave under the assumptions:

- no interference between signals from the same receiver with different paths of propagation,
- no polarization change, and
- no electron density variation in the ionosphere during propagation.

B. EXTENDING PREDICTED DATA

1. Signal power

The predicted field strength from IONCAP is converted to received signal power using the gains of the specific transmitting and receiving antennas, using the formulas (Ref. 6)

$$P = P_a A_e, \tag{2.1}$$

$$P_a = E^2/120\pi, \quad \text{and} \tag{2.2}$$

$$A_e = (\lambda^2/4\pi)G_{rc}, \tag{2.3}$$

where

P is the signal power at the receiver input in W,

P_a is the power flux in W m^{-2},

E is the electric field strength at the receiver input in V m^{-1},

A_e is the effective aperture of the receiving antenna in m^2,

λ is the wave length in m, and

G_{rc} is the gain of the receiving antenna for the predicted receiving angle.

Combining the above, formulas we get

$$P = (E^2/120\pi)(c/f)^2(G_{rc}/4\pi), \tag{2.4}$$

where

c is the speed of light, and

f is the frequency.

The field strength, E, in (2.4) must include the gain of the transmitting antenna for the take-off angle (TOA). Including this gain, the final formula in dBW becomes

$$P = E_{ion} + G_{tr} + G_{rc} - 20\log(f_m) - 107, \qquad (2.5)$$

where

E_{ion} is the predicted field strength by IONCAP in dB above μV/m,

f_m is the frequency in MHz, and

G_{tr} is the gain of the transmitting antenna for the predicted TOA.

The gains for the transmitting and receiving antennas are calculated with the aid of NEC (Appendix B). Because IONCAP is used with a constant gain antenna (8 dBi) the G_{tr} in (2.5) must be reduced by 8 dB.

2. Noise Power

The noise power at the receiver input is given by

$$N = KTBF_a, \qquad (2.6)$$

where

N is the noise power at the receiver input in Watts,

K is Boltzman's constant ($1.374*10^{-23}$ joules / ° Kelvin),

T is the temperature at the receiver in ° Kelvin,

B is the bandwidth of the receiver in Hz, and

F_a is the noise figure.

Using T=290° K and bandwidth B=50 Hz (Ref. 3) and converting the (2.6) to dBW we get

$$N = -204 + 20\log(B) + F_a. \qquad (2.7)$$

The F_a is frequency dependent. Curves for man-made and atmospheric noise are depicted in Figure 1 (Ref. 7). The suburban man-made noise is considered to be the predominant noise factor in the HF spectrum at the receiving position (Leicester UK).

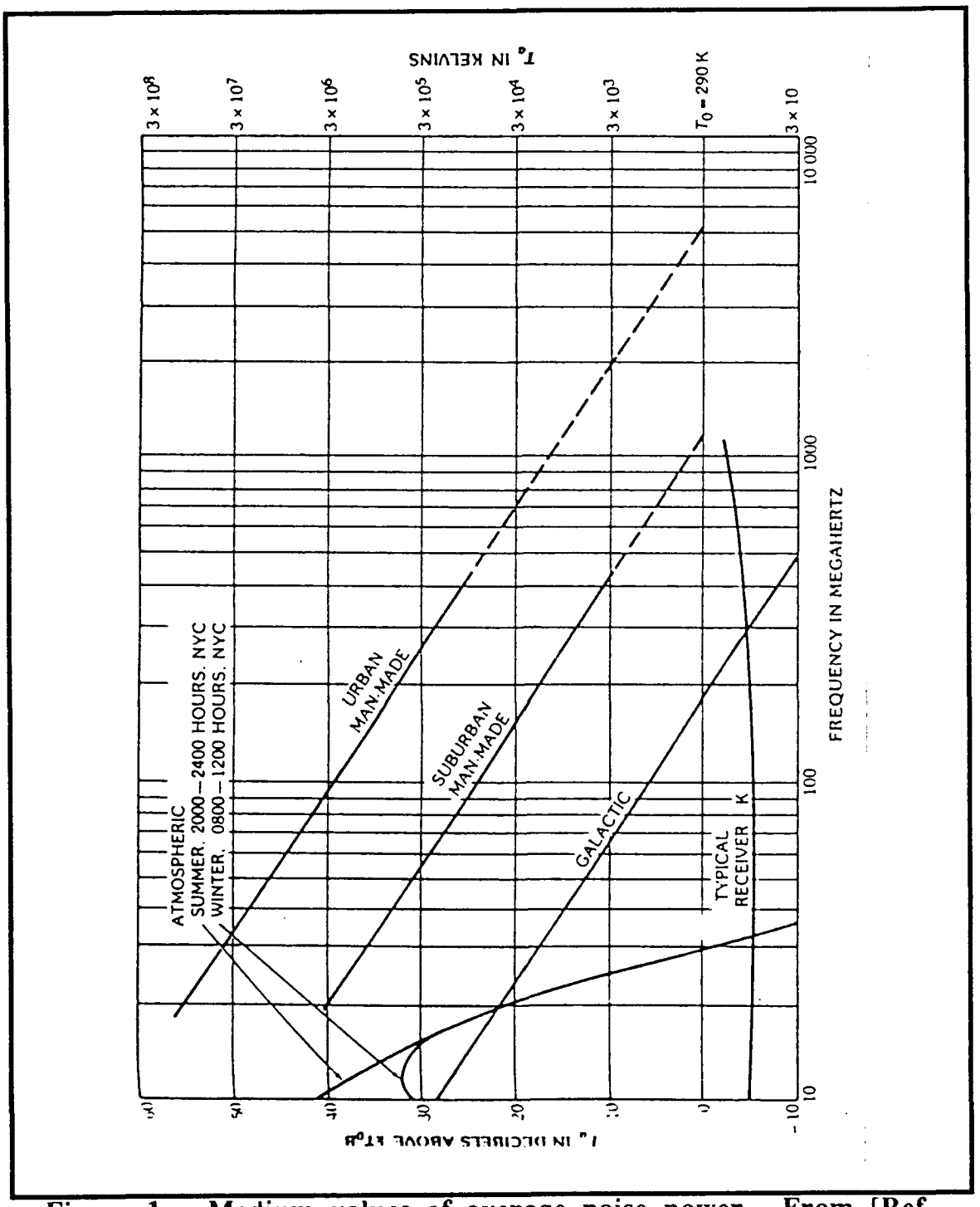

Figure 1. Medium values of average noise power. From [Ref. 7:p.34-9]

III. ANTENNA MODELING

The two transmitting antennas (the Butternut and the elevated whip) that were used at Clyde River, Canada, were modeled using the Numerical Electromagnetics Code , version 3 (NEC-3).

NEC is a computer program for the analysis of the electromagnetic response of antennas, developed at the Lawrence Livermore Laboratory, under the sponsorship of the Naval Ocean Systems Center and the Air Force Weapons Laboratory. It numerically solves the current integral equation for an antenna using the method of moments and produces current distribution, gains, input impedance, and other parameters.

The antenna modelling described here is based on the geometric dimensions. The gains used by the prediction model are included in Appendix B.

A. THE BUTTERNUT ANTENNA

The HF6V Butternut trap-vertical monopole antenna was used in the summer '88 campaign. It is a broadband HF antenna containing tuning traps with an adjustable height of 7.8 meters.

Three models are used in NEC for the above antenna, depending on the frequency. First, between 2 and 10 MHz, a series inductive base load reduces the capacitive input reactance. The height of the antenna is 7.8 meters and the feed point is near the ground. In the second model, which covers frequencies between 10 and 20 MHz, one end of the antenna is buried one meter below the ground. The above-ground height is 7.2 meters. The input impedance increases

with frequency. The third model, for frequencies 20 MHz and above, is modeled with a height of 7.05 meters and an excitation point 3.3 meters above the ground. The feed point input resistance varies substantially with frequency. Figure 2 depicts the input resistance versus frequency. The radiation patterns for the above three cases are depicted in Figures 3, 4, and 5.

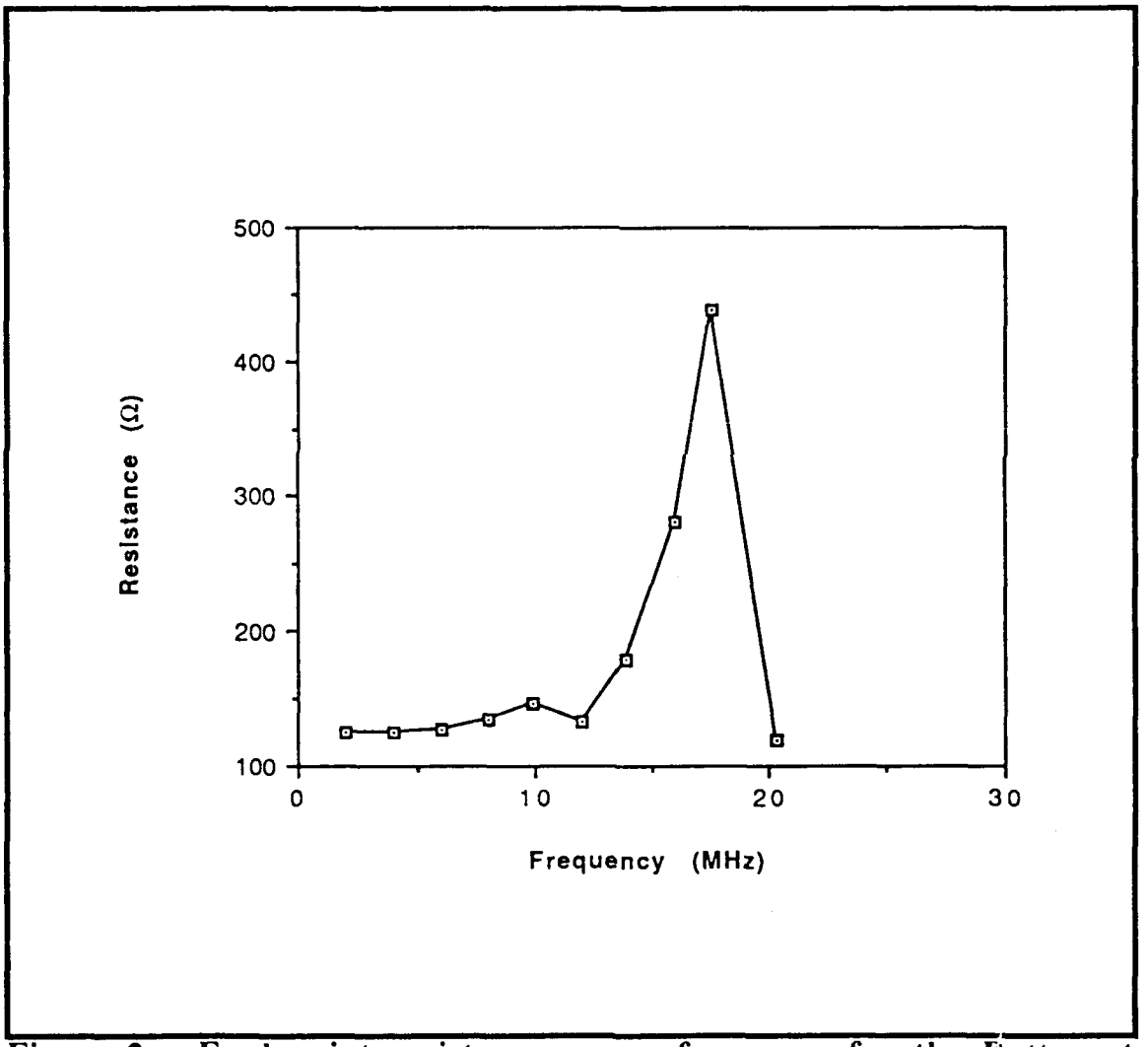

Figure 2. Feed point resistance versus frequency for the Butternut trap-vertical monopole antenna.

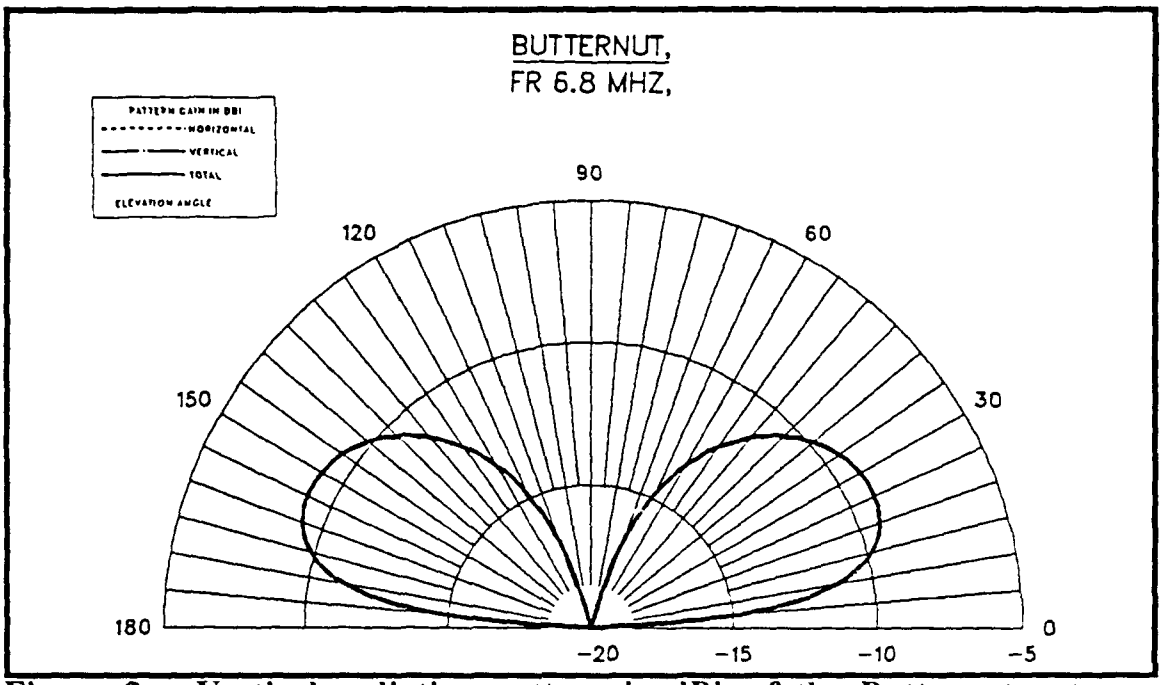

Figure 3. Vertical radiation pattern in dBi, of the Butternut antenna model 1, at 6.8 MHz.

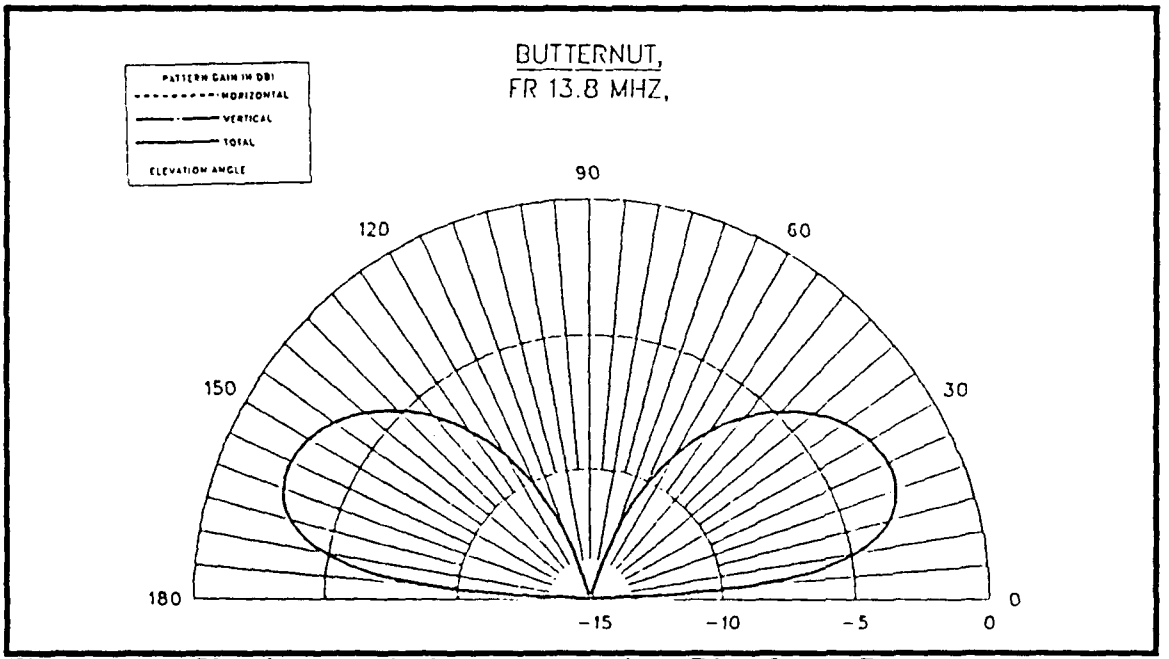

Figure 4. Vertical radiation pattern in dBi, of the Butternut antenna model 2, at 13.8 MHz.

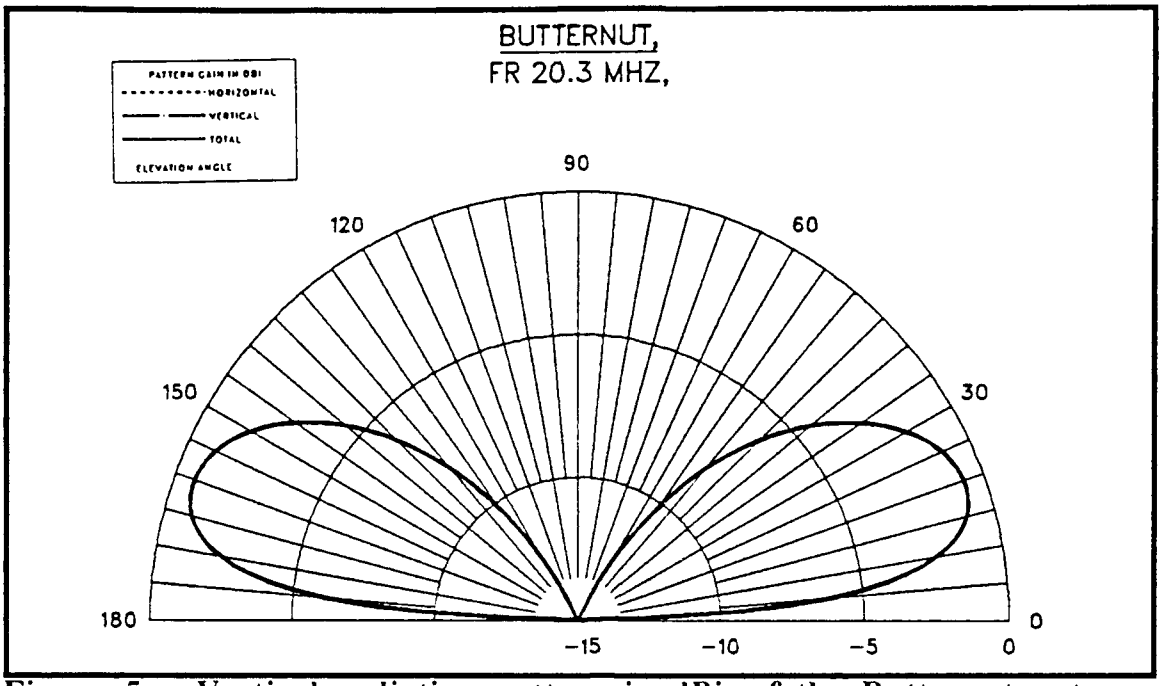

Figure 5. Vertical radiation pattern in dBi, of the Butternut antenna model 3, at 20.3 MHz.

B. THE WHIP ANTENNA

The XWB/V-2000 whip antenna was used in the winter '89 campaign. It is a broadband HF 7-meter vertical antenna designed to operate 5 meters above the ground in order to give a 2:1 VSWR or less. It is appropriate for long-range skywave communications and short range ground wave operation

The antenna is a 7-meter rod with an elevated feed point at 5 meters above the ground. Broadband input impedance is achieved by swamping-out impedance variations by a parallel resistive load, reducing gain, but maintaining reasonable driving-point impedance. Because of the arctic tundra during the winter in Clyde River, the values of relative permittivity (ε) and conductivity (σ)

of the ground beneath the antenna are functions of frequency. Table 3 in Appendix B shows the values that are used in the model (Ref. 8). The calculated input impedance versus frequency and a typical radiation pattern are depicted in Figures 6 and 7, respectively.

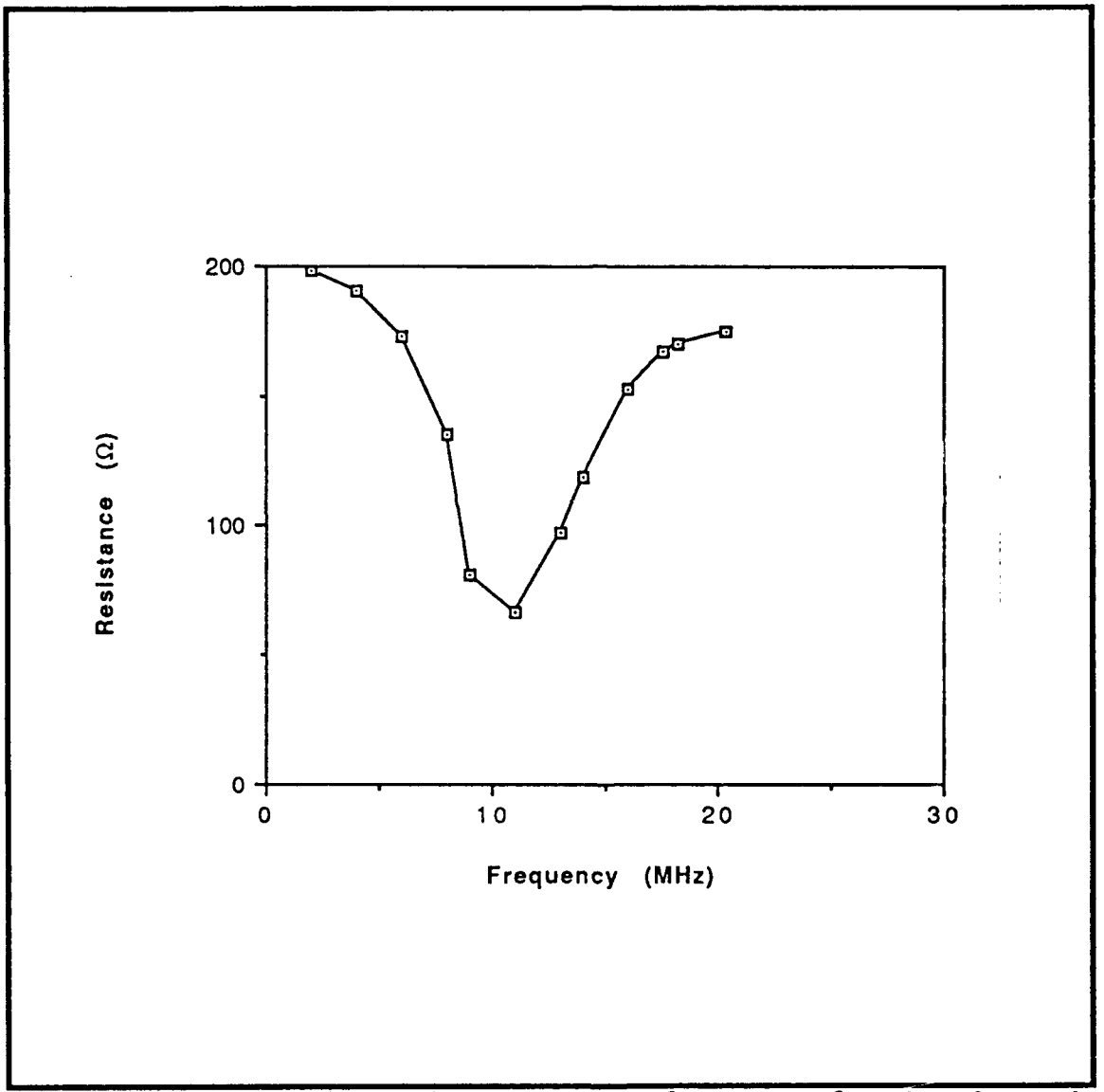

Figure 6. Feed point resistance versus frequency for the elevated whip antenna.

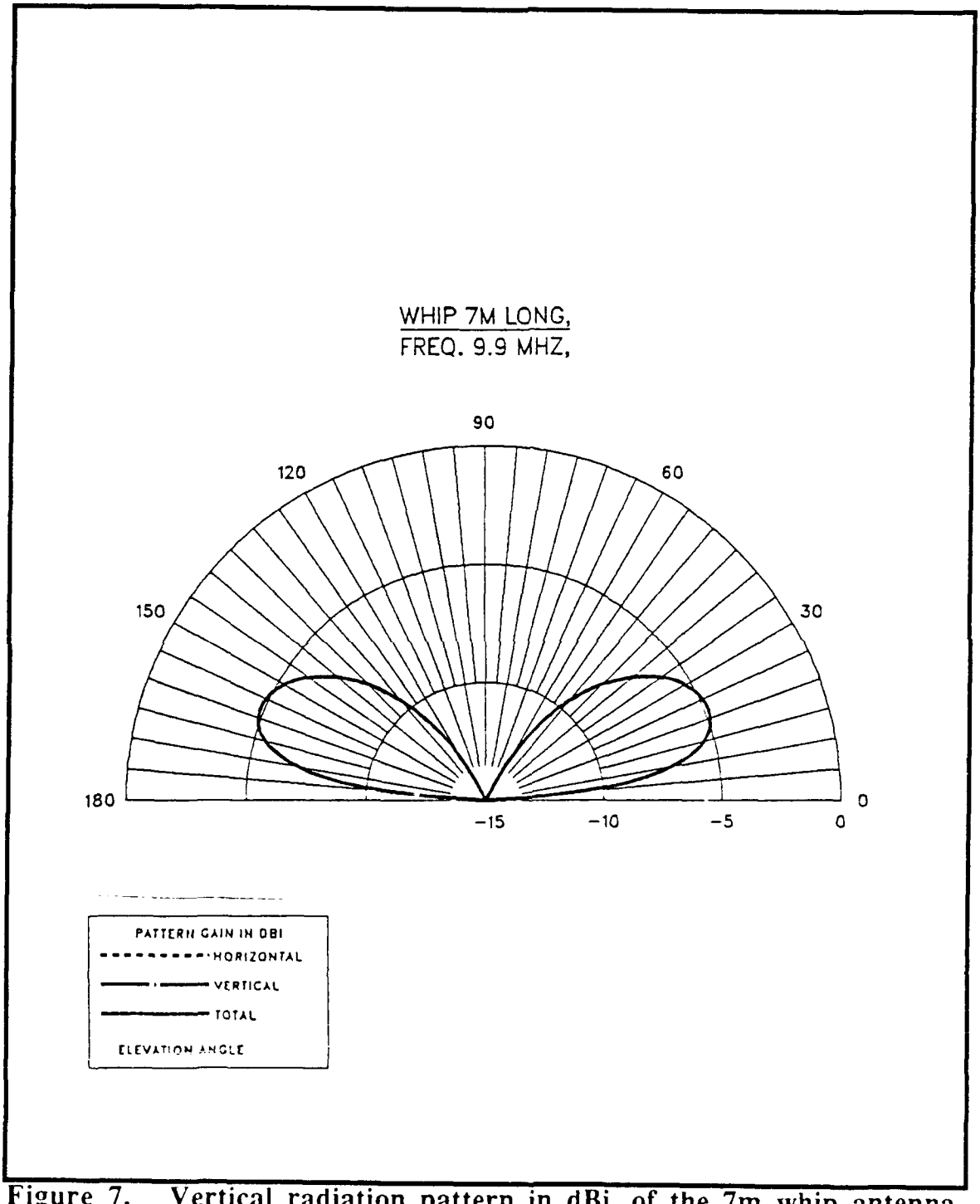

Figure 7. Vertical radiation pattern in dBi, of the 7m whip antenna at 9.9 MHz.

IV. COMPARISON OF IONCAP-PC 2.5 PREDICTIONS WITH THE NONCENTRIC DATA

A. NONCENTRIC DATA

The noncentric data used for comparison with IONCAP-PC 2.5 predictions were collected during the summer 1988 and winter 1989. The transmitting location was at Clyde River, Canada and the receiving station was at Leicester, UK. The peak value from a 1000 point FFT was listed as the signal level in the database. The spectrum was 50 Hz (-25 to 25 Hz). The noise level was calculated for the interval -25 to -12.5 Hz and then this value was assumed to represent the mean value for the whole spectrum. In order to speed up the analysis of the noncentric data and remove the need for manual examination of the data, two tests were used which were developed by the University of Leicester to determine the presence of a noncentric signal (Ref. 2). The tests are based on a) the Doppler spreading of the CW transmission, and b) the recognition of the call sign.

Signals that passed both tests were used as reference data for comparison with IONCAP-PC 2.5. The two signal-recognition tests were evaluated by comparing the results to manually-produced ones. The comparison gave the same results 80-90% of the time (Ref. 2).

The noncentric data were received in ASCII files. The received files include the following information:

- frequency,
- hour,

- minute,
- day,
- date,
- month,
- year,
- peak signal level,
- noise measured in the same units as signal level, and
- spread index.

The summer '88 campaign includes thirteen frequencies collected during twenty five days from 17 July through 12 August. The winter '89 campaign includes the same thirteen frequencies, collected in twenty-five days from 18 January through 12 February. Six of the thirteen frequencies for each campaign were selected for comparison. The selection for both campaigns was based on the number of data per frequency and for a representative coverage of the HF spectrum. The SNR of the data was obtained by subtracting the noise from the peak signal level in dB. A total number of 2,225 SNR measurments were calculated for both campaingns using LOTUS 1-2-3.

B. PREDICTED DATA

Input parameters for IONCAP-PC 2.5 are the sunspot number for each day, month, year and gain for transmitting and receiving antennas. The sunspot numbers were obtained from Ref. 9. The field strength output of IONCAP-PC 2.5 was corrected for the actual transmitting and receiving antenna gains and then converted to signal power as described in Chapter II. Subtracting the noise power from the signal power in dB for each frequency respectively, the

predicted SNR was derived. This procedure was applied to each of the 2,225 field strength outputs of IONCAP-PC 2.5 for the two campaigns.

C. ANALYSIS OF PREDICTION ERROR

The prediction error is obtained by subtracting the noncentric SNR from the predicted one. It is a measure of how well the predicted data matches the noncentric data. The statistical analysis is based on finding the error frequency distribution and the cumulative error frequency distribution. Because the noncentric data are measurments at the receiver after an RF distribution system, the unknown additional noise and interference of this system make the direct comparison between noncentric and predicted data impossible In order for the data to be referenced to a common point, making some comparison possible, the mean value of the prediction error can be set to 0 for each campaign. For the summer '88 and winter '89 campaigns the mean value of the prediction errors between IONCAP-PC 2.5 and the noncentric SNR were -35 dB and -34 dB, respectively.

1. Summer '88 campaign

Figure 8 depicts the frequency distribution of the prediction error of the 1101 data points from summer 88 campaign. It is skewed and has a standard deviation of 18.9 dB. Twenty three percent of the data shows no error. The maximum percentange , 28%, shows 10 dB prediction error. Figure 9 depicts how the standard deviation varies with the 6 frequencies. It shows a minimum of 11 dB at 20.3 MHz and a maximum of 25.5 dB at 10.2 MHz. The standard deviation of the error drops as the frequency increases. Figure 10 depicts the cumulative error frequency distribution. Fifty percent of the data shows less than 10 dB prediction error and 85% shows less than 20 dB.

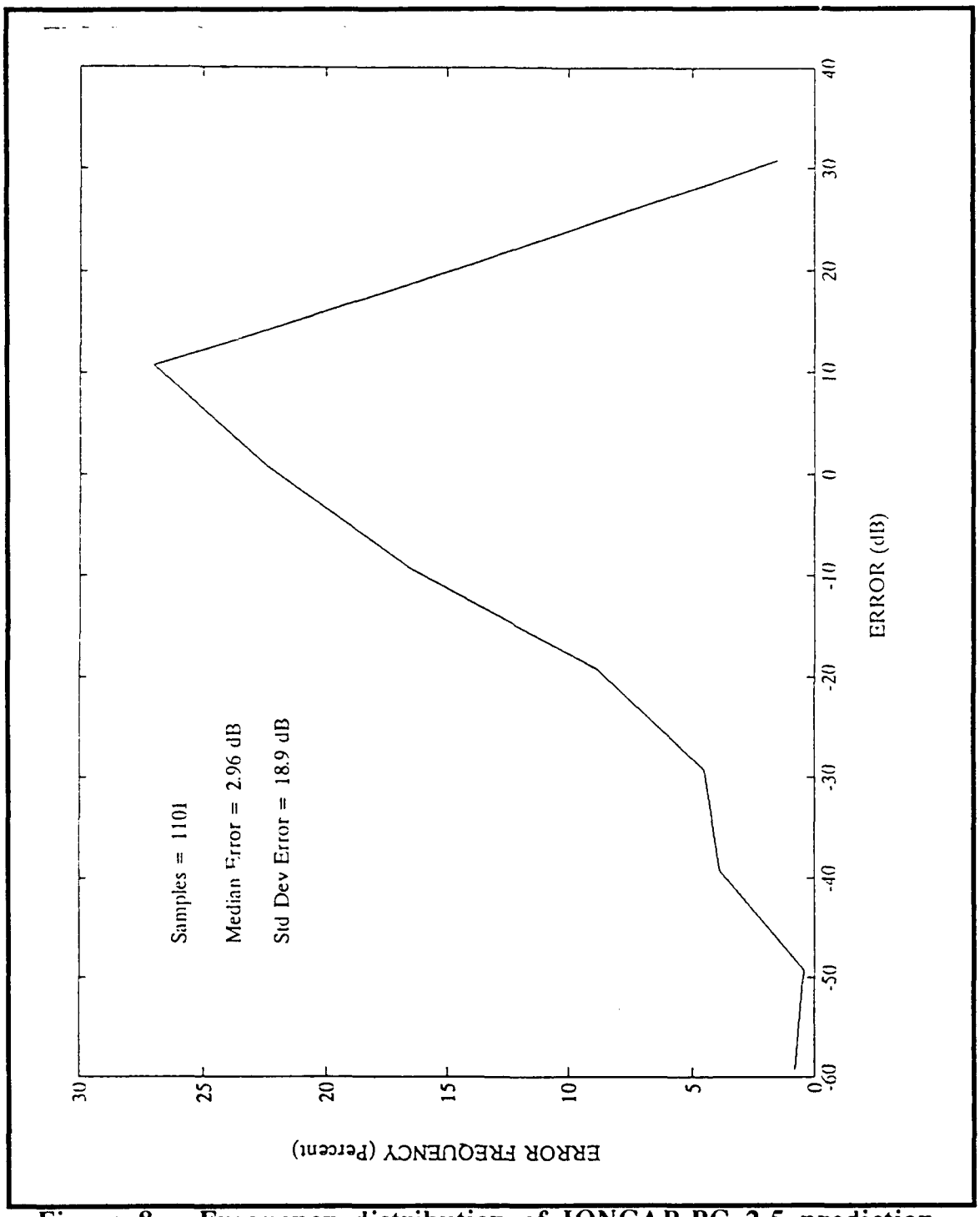

Figure 8. Frequency distribution of IONCAP-PC 2.5 prediction errors for the summer '88 campaign.

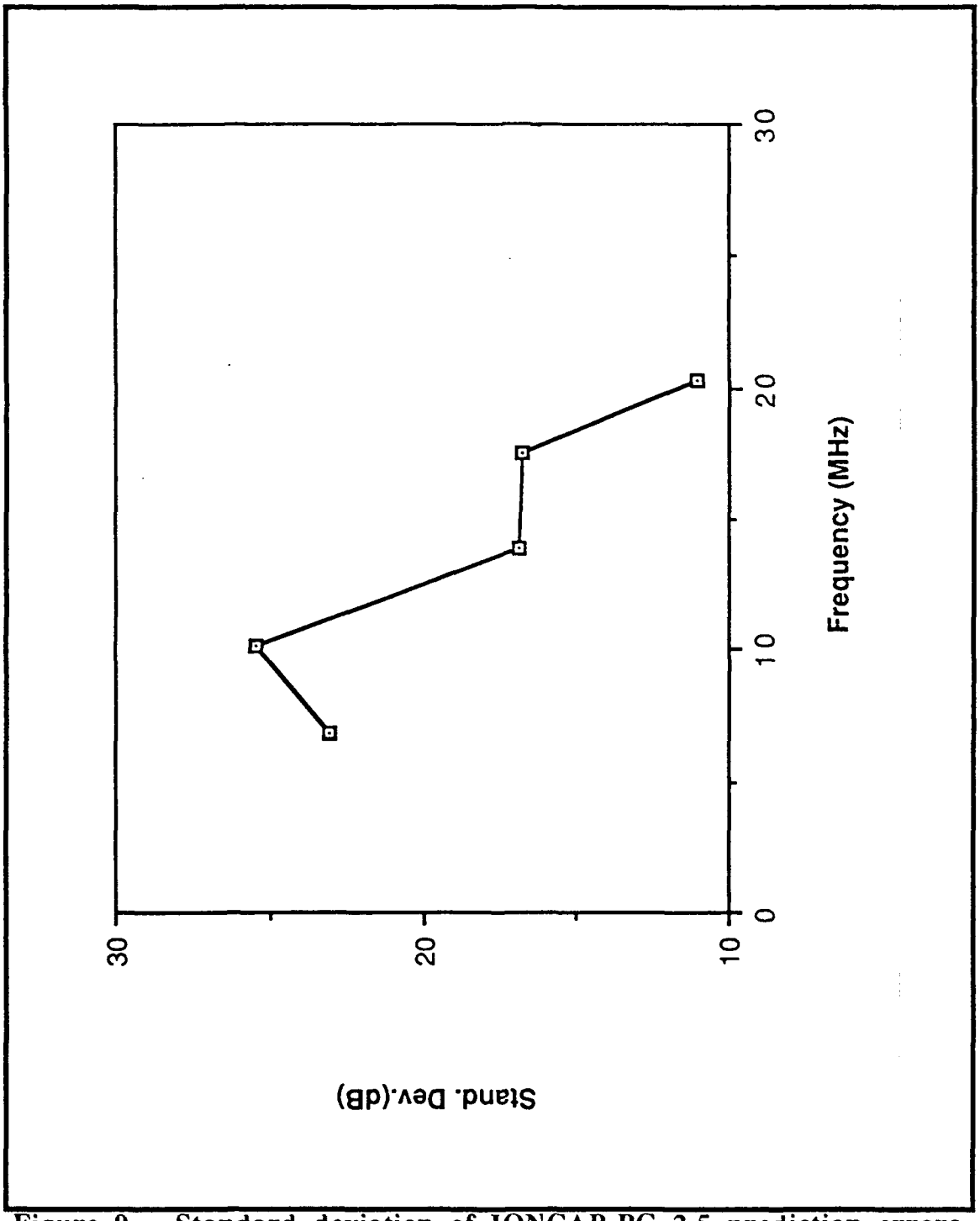

Figure 9. Standard deviation of IONCAP-PC 2.5 prediction errors versus frequency for the summer '88 campaign.

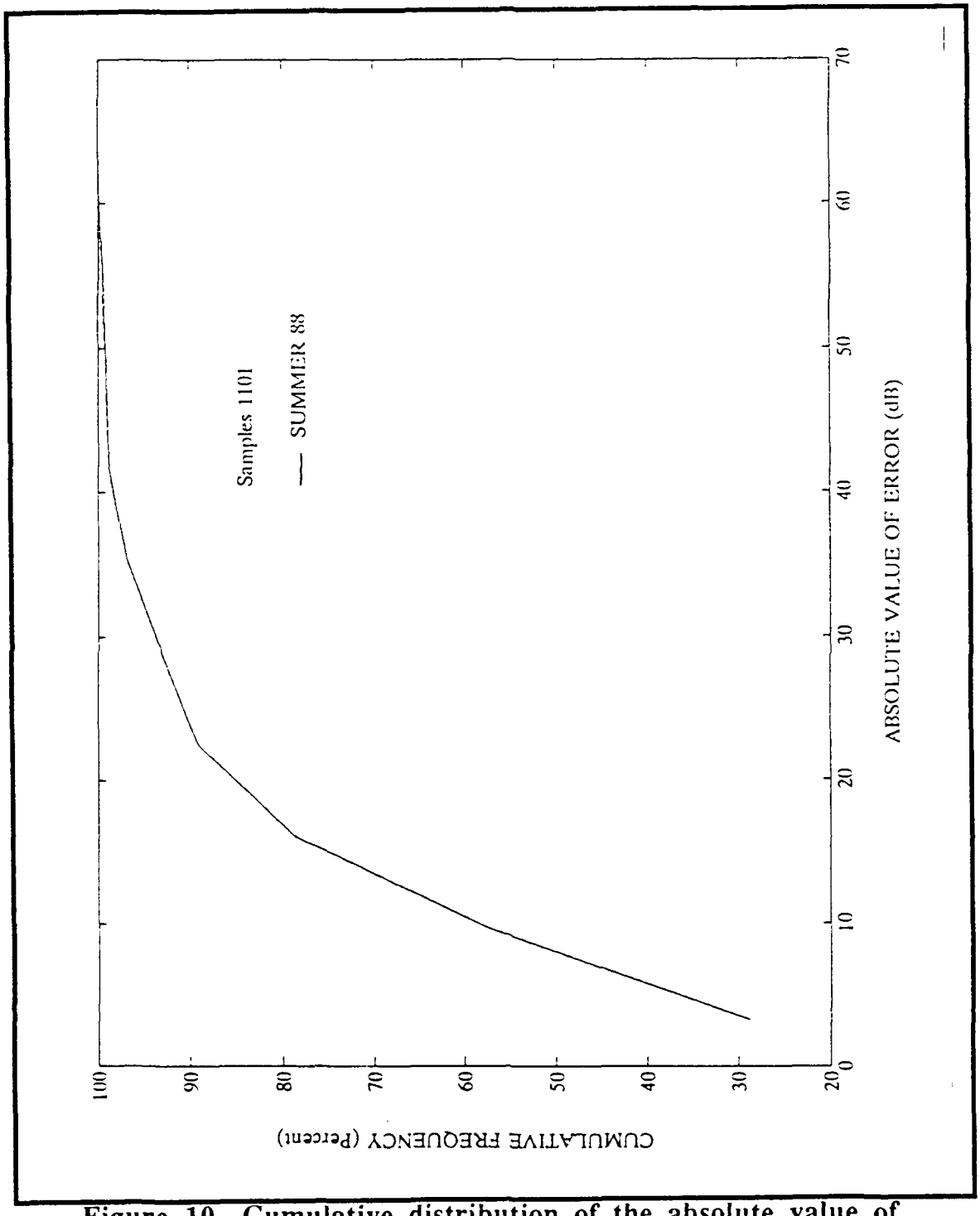

Figure 10. Cumulative distribution of the absolute value of IONCAP-PC 2.5 prediction errors for the summer '88 campaign.

2. Winter '89 campaign

Figure 11 depicts the prediction error frequency distribution of 1124 data points from the winter '89 campaign. It is similarly skewed and has a standard deviation of 18.5 dB. Only twenty three percent of the data shows no prediction error. The peak value of the prediction error, for 33% of the data, occurs at 18 dB. There are some prediction errors over -60 dB. This happens because IONCAP-PC 2.5 predicts median values of field strength and it is impossible to follow the extreme values of noncentric data. Figure 12 depicts how the standard deviation varies with the 6 frequencies used in the campaign. It shows a minimum value of 8.7 db at 9.9 MHz and a maximum of 20.3 dB at 17.5 MHz. Figure 13 depicts the cumulative error frequency distribution. Fifty percent of the data shows less than 10 db prediction error and 85% shows less than 20 dB.

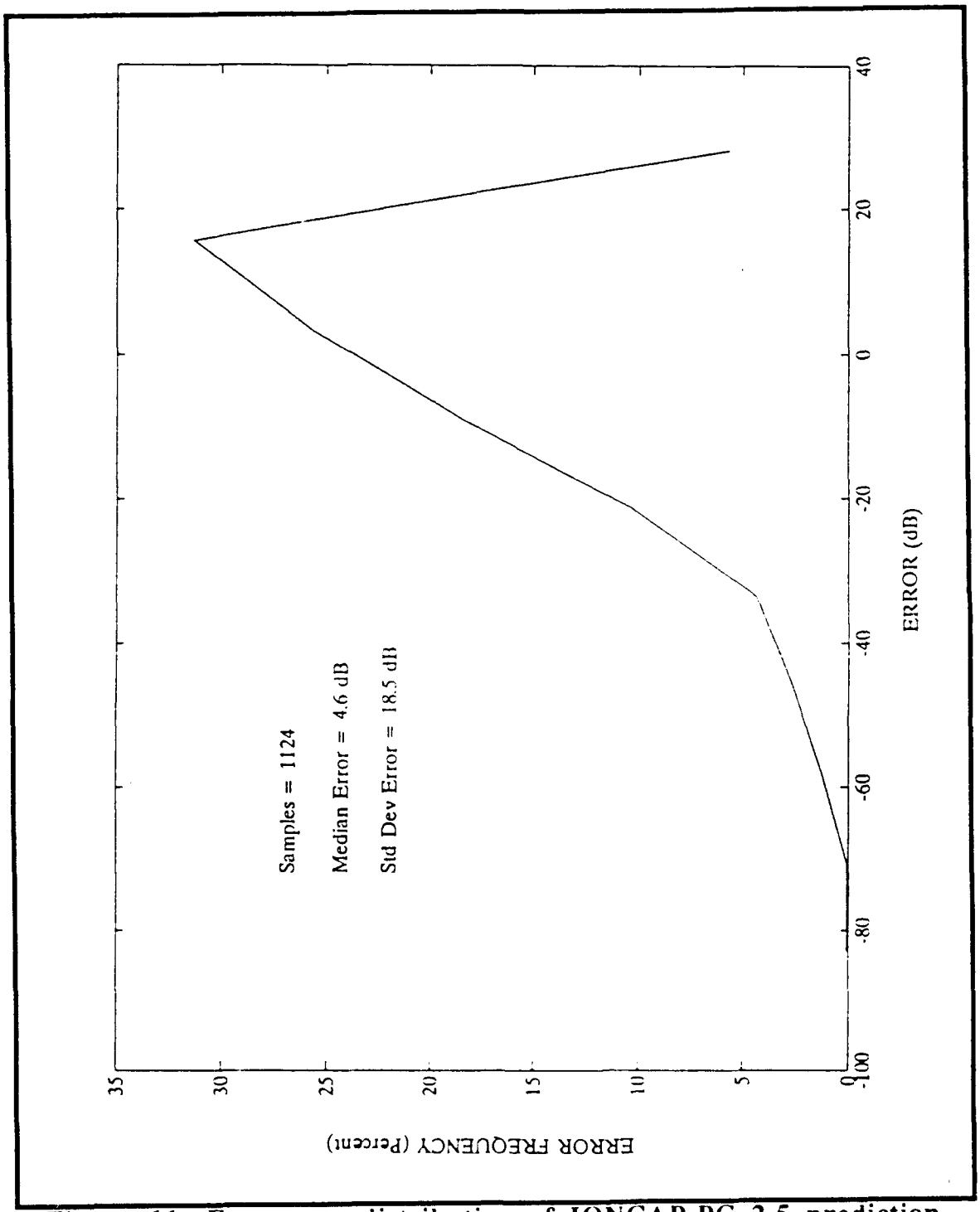

Figure 11. Frequency distribution of IONCAP-PC 2.5 prediction errors for the winter '89 campaign.

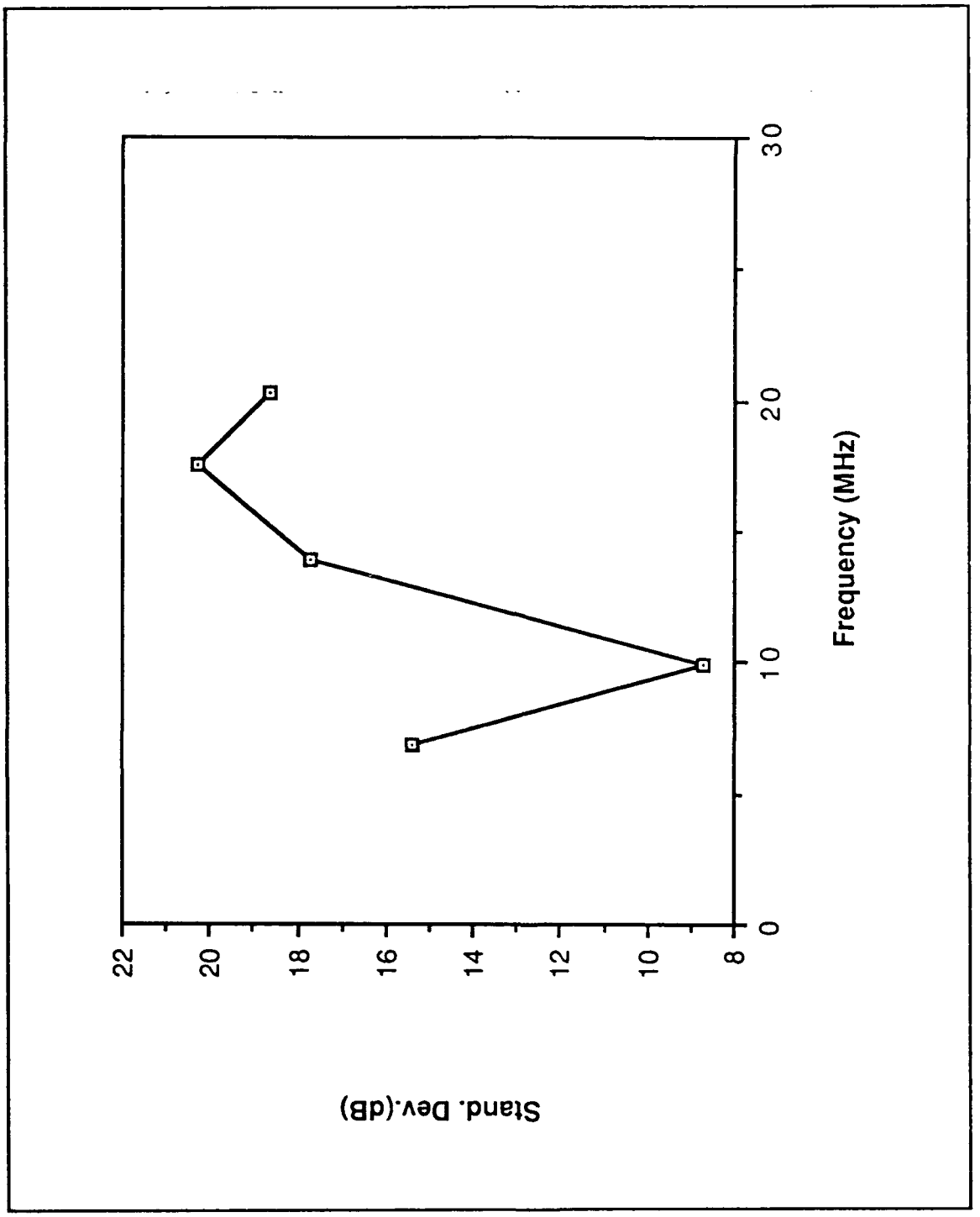

Figure 12. Standard deviation of IONCAP-PC 2.5 prediction errors versus frequency for the winter '89 campaign.

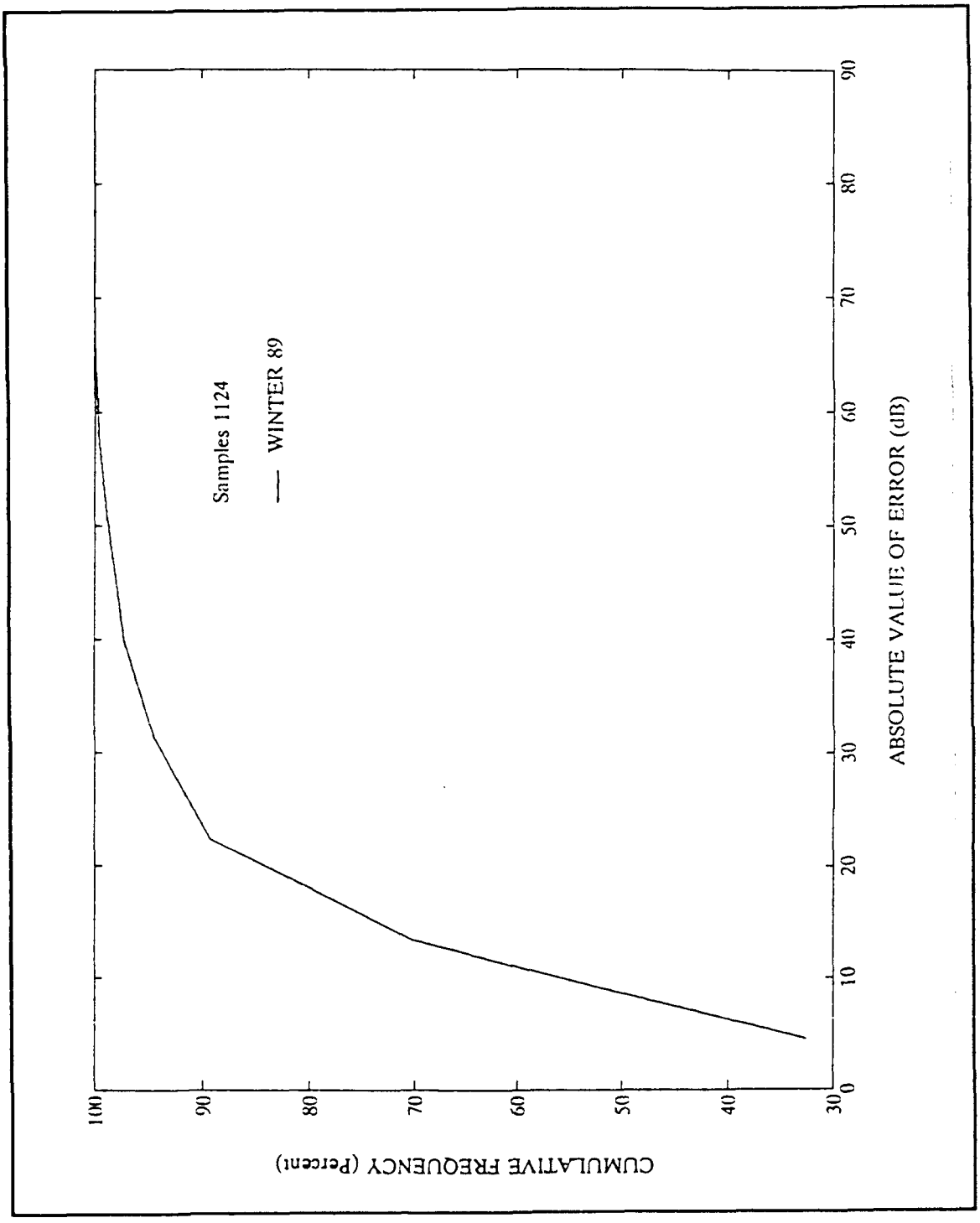

Figure 13. Cumulative distribution of the absolute value of IONCAP-PC 2.5 prediction errors for the winter '89 campaign.

3. Summer 88 - Winter 89 comparison

Figure 14 depicts the cumulative error frequency distributions of both campaigns, showing very similar distributions. The small amount of data with no error can be explained by the fact that IONCAP-PC 2.5 predicts median values of field strength. In summer '88 campaign, less prediction error at higher frequencies than at lower ones (Fig. 9). In the winter '89 campaign the opposite occurs. Lower frequencies show less prediction error than higher frequencies. This result was expected because high MUFs occur for more hours per day in summer than in winter.

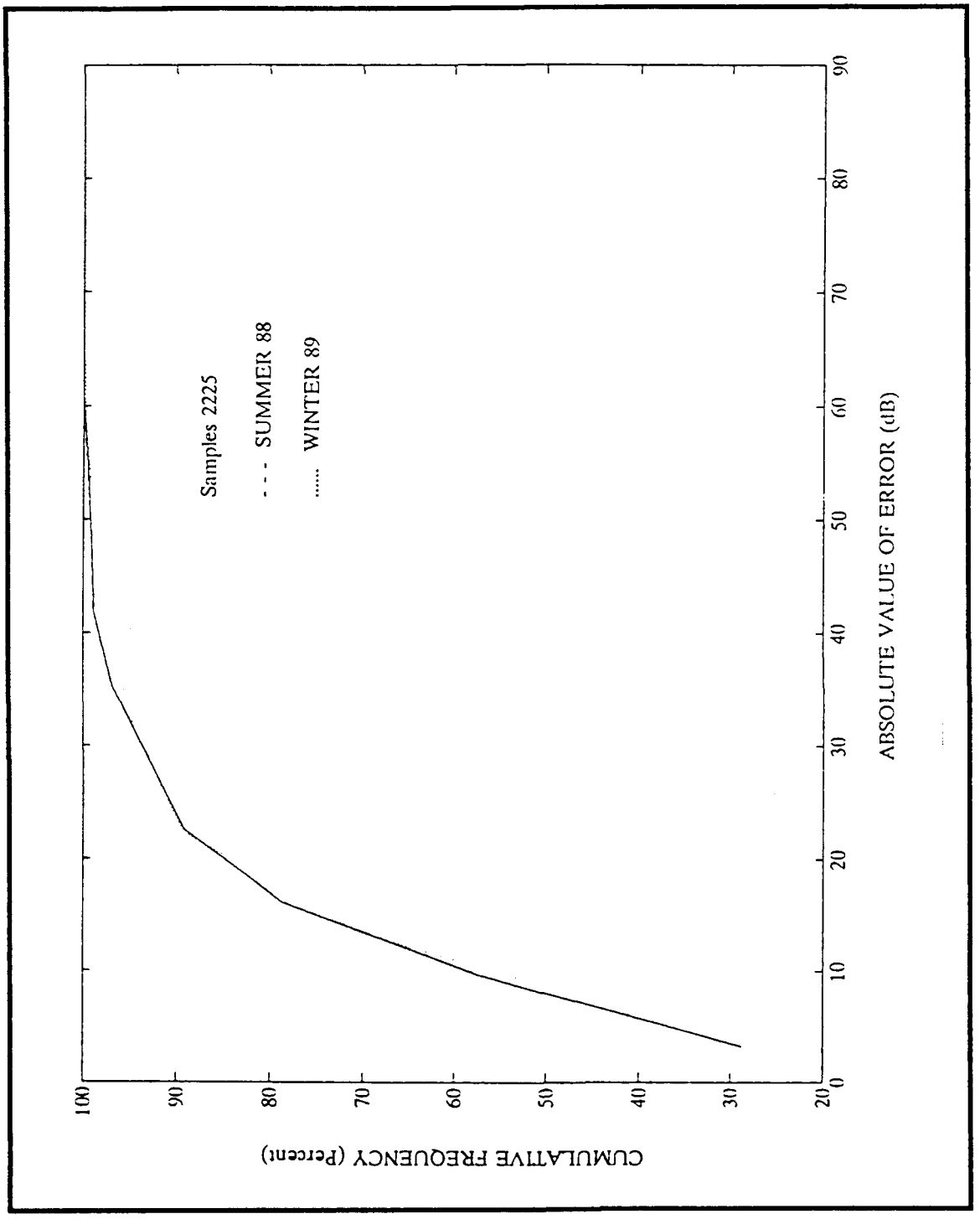

Figure 14. Cumulative distributions of absolute value of IONCAP-PC 2.5 prediction errors of both campaigns.

V. CONCLUSIONS AND RECOMMEDATIONS

A. CONCLUSIONS

Comparison of IONCAP-PC 2.5 predicted SNR with the noncentric data shows that IONCAP is not very accurate for the transpolar communication link tested. Such performance was expected from IONCAP-PC 2.5. It predicts median values of field strength, and therefore, when large variations in field strength occur, as happens in the polar regions due to various disturbances in the ionosphere at these latitudes, these predictions are likely to be inaccurate. This is the reason ITS has just developed a specific ionospheric prediction computer program, ICEPAC, for polar regions. This research examined whether the existing IONCAP, designed for mid-latitudes would provide useful results for high latitudes.

B. RECOMMEDATIONS

A similar comparison between ICEPAC and the same noncentric data is necessary and is underway at the Naval Postgraduate School (NPS). IONCAP-PC 2.5 can also be exercised on additional transpolar paths in the noncentric database to see if the results of this study apply to other polar circuits.

Any data to be used in future comparisons with ionospheric prediction programs must be collected in a manner that eliminates the uncertainty discovered in the noncentric data. Since ionospheric predictions produce field strength values, measured data must relate directly to field strength, and should not include the effects of receiving site RF distribution systems. Future

measurment programs should locate receivers and transmitters at sites which cover all possibilities of locations within the polar cap, under the auroral oval, in the auroral trough and below the polar regions.

APPENDIX A IONOSPHERIC PROPAGATION BACKGROUND

A. THE IONOSPHERE

We can divide the sources of energy in the ionosphere into the following categories:

1) solar radiation in the extreme ultraviolet (EUV) and X-ray ranges of the spectrum,
2) charged particles (mainly electrons) associated with aurora phenomena,
3) meteorites travelling through the atmosphere,
4) protons and alpha particles emmitted from the sun mainly during cromospheric eruptions (solar flares), and
5) galactic cosmic rays.

Among the above categories, cases (2) and (4) have the greatest effect on high latitude regions (above 60°).

As energy impinges from the sun on the upper part of the earth's atmospere, it ionizes (creates ion-proton pairs) the atmospheric gases. The ions and electrons are involved in a further interaction among themselves as well as an interaction with the neutral particles, which results in recombination and the creation of new ions and electrons. From a communications point of view, electron density is the most important factor. This is because the EM wave interacts more with the fast moving electrons than with heavier and slower ions.

The continuity equation which describes the density of electrons is

$$dN/dt = q - L - \mathrm{div}(N\hat{u}), \qquad (1)$$

where

N is the electron density,

q is the production rate of electrons,

L is the loss rate due to electron-ion recombination, and

$\hat{u}$ is the electron horizontal shift velocity.

The quantity q in equation (2.1) is a function of the energy source, the cross section under consideration, and the concentration of atoms or molecules.

Chapman (1931) was first to give an electron density rate function (q), with certain assumptions, although he took into account only the intensity of solar radiation. One must take into account the contribution by the production rate and other energy sources as well. The electron loss rate by recombination (L) depends on the square of concentration

$$L=aN^2, \qquad (2)$$

where a is the recombination coefficient, and under the assumption that only neutral particles result from the recombination. If we assume that negative ions are also created, the loss rate is given by

$$L=bN, \qquad (3)$$

where b is called the attachment coefficient. The final term, div(Nû), in the continuity equation (1), describes the movement of plasma into and out of the volume under consideration

Because the synthesis of the atmosphere is a function of height, absorption for each specific component of solar radiation occurs at a distinct height. It is generally accepted that the ionosphere consists of the following regions: D, E, F1 and F2, progressing from lower to higher altitudes, but the boundaries between these regions are not clear-cut.

1. D-Region

The D-region is the lowest (60-90 km). Its higher part is ionized by hydrogen Lyman-alpha of Solar radiation and the lower part by cosmic radiation. The D-region disappears at night and is responsible for energy absorption of MF and lower HF radio waves.

The D-region is succeptible to sudden ionospheric disturbances (SID). Solar X-rays, due to the occurance of solar flares, penetrate into the region and result in an increase of the electron density. SIDs last about half an hour.

Polar cap absorption events (PCAs) are also observed in the D-region. Interaction between the geomagnetic field and the interplanetary magnetic field (IMF), which is brought to the earth by the solar wind, leaves the polar cap atmosphere open to charged particles (Fig. A1). Thus, protons and alpha particles of the solar wind enter at the Nothern and Southern parts of the atmosphere (approx. 78° latitude) and cause the so-called polar cap absorption. At polar regions the absorption of EM waves in the HF spectrum can be 100%.

This phenomenon occurs from one to several hours after a solar flare is observed.

A third type of disturbance in the D-region is due to auroral phenomenon. It occurs in an oval zone between 65° and 70° latitudes. High energy electrons from the auroral zone precipitate at high latitudes and produce extra ionization. These phenomena last from a minute to an hour.

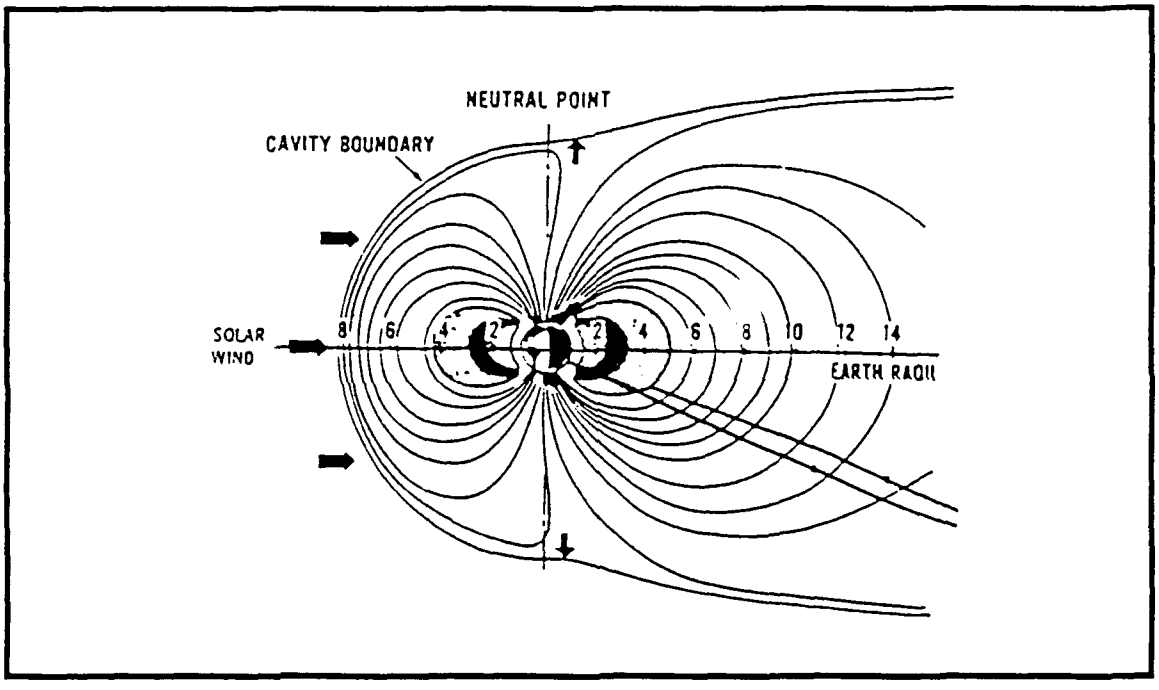

Figure A1. Earth's magnetic field showing the neutral points. From [Ref. 10: p.55]

At high latitudes in winter when the sun never raises the ionization source at heights under 70 km, galactic cosmic rays are found. During this period, there is only small diurnal variation in the electron density. During the summer (July), when the sun never sets on the polar regions (Northern

hemisphere) there is diurnal variation. The peak diurnal variation is observed in March.

2. E-Region

The E-region covers the altitudes between 90 to 140 km. Soft X-rays and EUV radiation from the sun are absorbed in this region. It is one of the regions where ionospheric *reflection* occurs. The lower part of this region is succeptible to the same disturbances as the D-region at high latitudes.

At the same altitude of the E-region a moving, high-electron-concentration layer is observed from time to time. It is about 2 km thick and moves with a mean velocity of 110 km/h. This layer is called sporadic-E (E_S). The cloudlike E_S strongly absorbs the EM waves in the HF range.

3. F-Region

The F-region is divided in two subregions (F1 and F2) during the day and is the main "reflector" for HF radiation. Solar EUV radiation produces the F1-region above 140 km. The peak of electron density is observed at 160 km during the day. During the night the F1-region merges with the F2. The F2-region normally shows maximum ionization of all the regions, even though at 300 km (where the peak value of electron density occurs), there is no peak absorption for EM radiation. An explanation is that at this specific height the recombination rate of electrons is less than the ion electron production and, on the other hand, diffusion produces an electron density distribution which decreases with height.

B. SKY WAVE PROPAGATION

1. Basic Definitions

EM waves in the HF spectrum, transmitted from the ground to the sky (sky waves) penetrate the ionsphere where they are subjected to progressive refraction. This happens because, as they increase in height, they encounter ionospheric regions with increasing electron density. As the refraction index increases with height, the EM waves change direction, bending to back towards the earth. It is possible, depending on the frequency and the electron density of the ionosphere, for a sky wave to be "reflected" all the way back to the earth. The part of the HF spectrum will propagate at a given time is determined by the critical frequency, maximum usable frequency, and optimum working frequency, as discussed in the following sections.

a. Critical Frequency

The critical frequency is the maximum frequency which returns to the earth from the ionosphere when the transmission takes place vertically. The critical frequency (f_o) is a function of electron density (N) in the ionosphere

$$f_o=9N^{0.5}. \tag{4}$$

Because the sky wave can be reflected from either the E or F regions depending on the frequency, the critical frequency is labeled as f_oE, f_oF1, or f_oF2 respectively.

b. Maximum Usable Frequency (MUF)

If transmission takes place in other than a vertical direction, the maximum frequency that can be used for ionospheric propagation depends on the angle the sky wave forms with the perpendicular at the point of total reflection in the ionosphere. We can find this angle assuming that the sky wave travels on a straight line until the point of reflection. The incident angle is then the complement of the take-off angle at the transmitting antenna (Fig. A2).

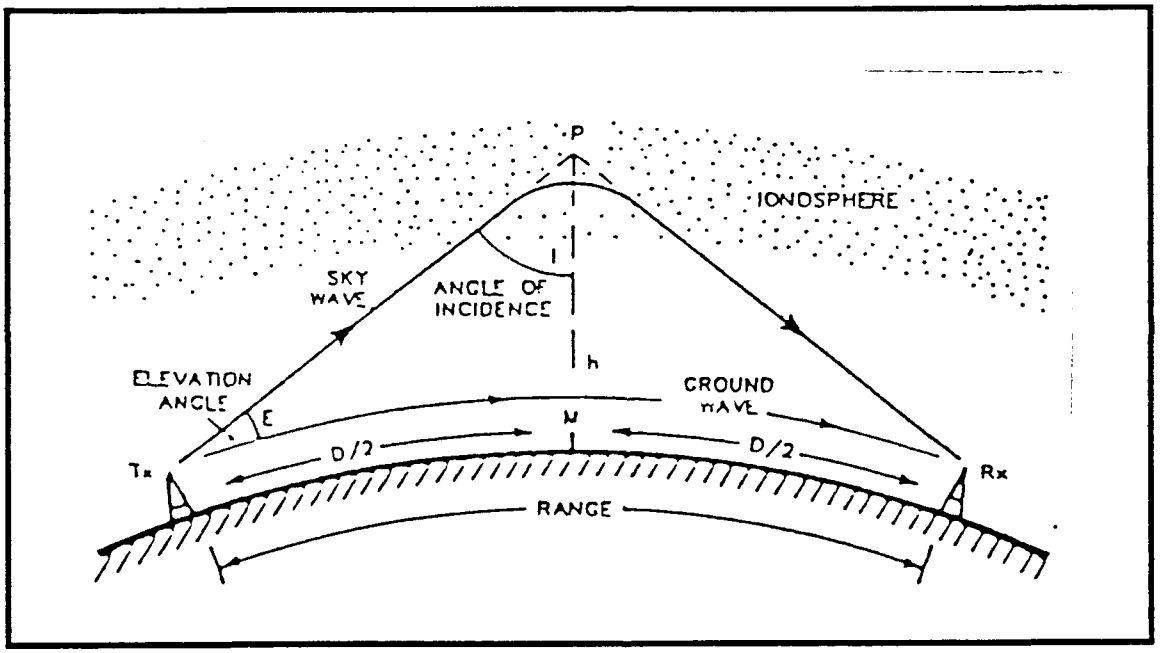

Figure A2. A simplified view of a path taken by skywave between transmitter (Tx) and receiver (Rx) showing the virtual height (h) and the angle of incidence (i). From [Ref. 11: p.84].

The above assumption uses a reflection point at a height higher than the actual reflection occurs. This imaginary height is called *virtual height*.

With the help of the virtual height the geometry of the propagation path is simplified. The relation for the MUF is given by

$$f_m = f_o \sec(i), \tag{5}$$

where i is the take off angle.

c. Lower Usable Frequency (LUF)

Even though the lower limit of the frequency of a EM wave reflected by the ionospere is not as sharply defined as the upper limit, one can define the LUF as the frequency below which communication is not reliable. The LUF is transmitter power dependent and the decrease in reliability is due to the increased ionospheric absorption as the frequency falls below the MUF.

d. Optimum Working Frequency (FOT)

It has been observed that when the communication path involves the F2 region, 90% of the time the MUF is higher than 85% of its median value. The FOT is defined as this value (85% of the F2-MUF). If the communication path involves reflection only in the E region, the FOT is the same as the MUF.

2. Path Loss

The loss of signal strength between transmitting and receiving antennas is called path loss. The path loss for a signal propagated through the ionosphere is determined by the following factors,

a. Free Space Loss

The free space loss is given by the relation

$$L_f = 20\log(4\pi d/\lambda), \tag{6}$$

where d is the distance and λ is the wavelength, both measured in the same units.

b. Ionosperic Absorption Loss

The absorption of the EM wave follows the same variations as electron density in the D-region and is called *non-deviative absorption.* Non-deviative absorption begins after sunrise and drops after sunset. It is greater in summer than in winter and generally depends on the sun's azimuth angle. When an EM wave is reflected almost vertically, an additional absorption is introduced and is called *deviative absorption.*

c. Polarization Coupling Loss

Depending on polarization, the EM wave propagates through the ionosphere in two distinctive modes. The first, called *ordinary wave,* occurs when the E-field polarization is linear and parallel to the earth's magnetic field. The other is called the *extraordinary wave* and occurs when the E-field is elliptically polarized on a level perpendicular to the earth's magnetic field. The extraordinary wave is highly absorbed and only the ordinary wave finally propagates.

d. Ground Reflection Loss

Ground reflection occurs in multi-hop mode propagation, when a signal reflected by the ionosphere, returns to the earth, is reflected back upward by the earth, and again by the ionosphere. Ground reflection loss refers to the signal loss upon this reflection by the earth, and depends on the dielectric constant and the conductivity at the reflection point.

e. Focus Gain

While the other factors mentioned describe the various ways in which a signal may be attenuated *focus gain* describes the increased signal strength due to the arrival of E/M waves at the receiver from not only one transmitting angle but from a cone of angles.

3. Variations of Ionosphere

Variations of the ionosphere which affect HF propagation are:

- diurnal (variation with solar zenith angle),
- seasonal,
- geographic and geomagnetic,
- solar activity, solar cycle and disturbances, and
- height (different regions).

APPENDIX B NEC DATA SET AND TABLES FOR ANTENNAS

A. BUTTERNUT ANTENNA (SUMMER 88)

1. First Data Set. Frequencies 2 to 10 MHz

```
CE BUTTERNUT
GW1,51,0.,0.,0.,0.,0.,7.8,.013,
GE-1,0,0,
FR0,1,0,0,6.8,0.,
GN2,0,0,0,10.,.01,
EX0,1,2,01,1.,0.,0.,
LD0,1,2,2,0.,0.86386E-4,0.,
RP0,91,1,1001,0.,0.,1.,0.,0.,0.,
EN
```

2. Second Data Set. Frequencies 10.1 to 20 MHz

```
CE BUTTERNUT
GW1,51,0.,0.,0.,0.,0.,7.2,.013,
GW2,9,0.,0.,-1.,0.,0.,0.,.013,
GE-1,0,0,
FR0,1,0,0,13.9,0.,
GN2,0,0,0,10.,.01,
EX0,1,4,01,1.,0.,0.,
LD0,1,1,1,0.,0.,0.,
RP0,91,1,1001,0.,0.,1.,0.,0.,0.,
EN
```

3. Third Data Set. Frequencies 20.1to 30 MHz

```
CE BUTTERNUT
GW1,51,0.,0.,0.,0.,0.,7.05,.013,
GE-1,0,0,
FR0,1,0,0,20.3,0.,
GN2,0,0,0,10.,.01,
EX0,1,22,01,1.,0.,0.,
LD0,1,1,1,0.,0.,0.,
RP0,91,1,1001,0.,0.,1.,0.,0.,0.,
EN
```

Table 1. BUTTERNUT ANTENNA GAINS (dBi)

Freq.(MHz) Angle(deg.)	6.8 & 6.9	10.2	13.9	17.5	20.3
1 - 3	-22	-19	-16	-14	-13
4 - 6	-15	-12	-9	-7	-6
7 - 9	-12	-9	-6	-4	-3
10 - 12	-11	-8	-4	-3	-2
13 - 15	-10	-7	-4	-2	-1
16 - 18	-10	-6	-3	-1	-1
19 - 21	-9	-6	-3	-1	-1
22 - 24	-9	-6	-3	-1	-1

B. WHIP ANTENNA (WINTER 89)

1. Data Set

```
CE WHIP
GW1,45,0.,0.,5.,0.,0.,12.,.02,
GW2,1,1000.,1000.,5.,1000.,1000.,5.1,0.02,
GW3,41,0.,0.,0.,0.,0.,5.,.02
GE-1,
FR0,1,0,0,13.9,0.,
GN2,0,0,0,9.,.002,
NT1,1,2,1,.005,0.,0.,0.,1E10,0.,
EX0,1,1,00,1.,0.,
RP0,91,1,1001,0.,0.,1.,0.,0.,
EN
```

Table 2. WHIP ANTENNA GAINS (dBi)

Freq.(MHz) Angle(deg.)	6.8 & 6.9	9.9	13.9	17.5	20.3
1 - 3	-29	-18	-18	-19	-18
4 - 6	-21	-11	-10	-12	-11
7 - 9	-19	-8	-7	-9	-9
10 - 12	-17	-7	-6	-8	-7
13 - 15	-16	-6	-5	-7	-7
16 - 18	-16	-5	-5	-7	-7
19 - 21	-15	-5	-5	-7	-7
22 - 24	-15	-5	-5	-8	-8

Table 3. VALUES OF RELATIVE PERMITTIVITY AND CONDUCTIVITY USED IN NEC MODELS OF WHIP ANTENNA.

FREQUENCY (MHz)	RELATIVE PERMITTIVITY	CONDUCTIVITY (S/M)
2-4	15	0.0012
6	12	0.0017
8	10	0.002
9	9.5	0.002
11-16	9	0.002
17	9	0.0024
18-20	8.5	0.0026

REFERENCES

1. *Ionospheric Communications Analysis and Prediction Program,* Institute of Telecommunication Sciences, Boulder, Colorado 80303, September 1978.

2. *Noncentric: Automatic Signal Recognition,* Ionospheric Physics Group, Leicester University, December 1989.

3. Messages received by FAX from Mike Warrington, Leicester University, 3 and 8 of August 1990.

4. S. S. Gikas, *A Comparison of High Latitude Ionospheric Propagation Predictions from Advanced PROPHET 4.0 with Measured Data,* MSEE Thesis, Naval Postgraduate School, Monterey, California, December 1990.

5. A. A. Tomko, *Statistical Analysis of the Prediction Accuracy of HF Propagation Models,* presented at the National Radio Science Meeting, Boulder, Colorado, January 1989.

6. Warren L. Stutzman and Gary A. Thiele, *Antenna Theory and Design,* John Wiley and Sons Inc., 1981.

7. Edward C. Jordan, *Reference Data for Engineers: Radio, Electronics, Computer and Communications*, Howard W. Sams and Company, seventh edition, 1989.

8. *Ground Constant Data,* private communications with George H. Hagn, 9-15-1990, SRI International, 164 N. Kent St., Arlington VA 22209.

9. *Journal of Geophysical Research*, American Geophysical Union, Vol. 93 and 94, 1988 and 1989.

10. Thomas D. Damon, *Introduction to Space The Science of Spaceflight,* Orbit Book Company Inc.,1990.

11. Leo Mc Namara and Roger Harrison, *Radio Communications Guide to the Ionosphere,* Australian Electronics Monthly, April 1986.

BIBLIOGRAPHY

1. K. Davies, *Ionospheric Radio Propagation,* National Bureau of Standards, April 1, 1965.

2. K. Davies, *Ionospheric Radio Waves,* Blaisdell Publishing Company, Boulder Colorado, May, 1968.

3. A. Picquenard, *Radio Wave Propagation,* N.V. Philips' Gloeilampenfabrieken, Eindhoven, 1974.

4. J. K. Hargreaves, *The High- Latitude Ionosphere: Geophysical basis,* Technical Literature Search, Naval Ocean Systems Center, San Diego, CA, January 1990.

5. J. K. Hargreaves, *The High-Latitude Ionosphere: Dynamical Aspects, and Models,* Technical Literature Search, Naval Ocean Systems Center, San Diego, CA, January 1990.